

1 **Accelerated Protein Biomarker Discovery from FFPE tissue samples**
2 **using Single-shot, Short Gradient Microflow SWATH MS**
3

4 Rui Sun^{1,2*}, Christie Hunter^{3*#}, Chen Chen⁴, Weigang Ge^{1,2}, Nick Morrice³, Shuang
5 Liang^{1,2}, Chunhui Yuan^{1,2}, Qiushi Zhang^{1,2}, Xue Cai^{1,2}, Xiaoyan Yu⁵, Lirong Chen⁵,
6 Shaozheng Dai⁶, Zhongzhi Luan⁶, Ruedi Aebersold^{7,8}, Yi Zhu^{1,2#}, Tiannan Guo^{1,2#}

7

8 1, Key Laboratory of Structural Biology of Zhejiang Province, School of Life Sciences,
9 Westlake University, 18 Shilongshan Road, Hangzhou 310024, Zhejiang Province, China

10 2, Institute of Basic Medical Sciences, Westlake Institute for Advanced Study, 18 Shilongshan
11 Road, Hangzhou 310024, Zhejiang Province, China

12 3, SCIEX, USA and UK (NM)

13 4, SCIEX, China

14 5, Department of Pathology, The Second Affiliated Hospital, Zhejiang University School of
15 Medicine, Hangzhou, Zhejiang, 310009, China

16 6, School of Computer Science and Engineering, Beihang University, Beijing, China

17 7, Department of Biology, Institute of Molecular Systems Biology, ETH Zurich, Switzerland

18 8, Faculty of Science, University of Zurich, Zurich, Switzerland

19 * co-first

20 # co-correspondence

21 **Emails:**

22 Christie Hunter: christie.hunter@sciex.com

23 Yi Zhu: zhuyi@westlake.edu.cn

24 Tiannan Guo: guotiannan@westlake.edu.cn

25

26

27 **ABSTRACT (no more than 4000 characters)**

28 We report and evaluated a microflow, single-shot, short gradient SWATH MS method
29 intended to accelerate the discovery and verification of protein biomarkers in clinical
30 specimens. The method uses 15-min gradient microflow-LC peptide separation, an optimized
31 SWATH MS window configuration and OpenSWATH software for data analysis.

32

33 We applied the method to a cohort 204 of FFPE prostate tissue samples from 58 prostate
34 cancer patients and 10 prostatic hyperplasia patients. Altogether we identified 27,976
35 proteotypic peptides and 4,043 SwissProt proteins from these 204 samples. Compared to a
36 reference SWATH method with 2-hour gradient the accelerated method consumed only 27%
37 instrument time, quantified 80% proteins and showed reduced batch effects. 3,800 proteins
38 were quantified by both methods in two different instruments with relatively high consistency
39 ($r = 0.77$). 75 proteins detected by the accelerated method with differential abundance
40 between clinical groups were selected for further validation. A shortlist of 134 selected
41 peptide precursors from the 75 proteins were analyzed using MRM-HR, exhibiting high
42 quantitative consistency with the 15-min SWATH method ($r = 0.89$) in the same sample set.
43 We further verified the capacity of these 75 proteins in separating benign and malignant
44 tissues (AUC = 0.99) in an independent prostate cancer cohort (n=154).

45

46 Overall our data show that the single-shot short gradient microflow-LC SWATH MS method
47 achieved about 4-fold acceleration of data acquisition with reduced batch effect and a
48 moderate level of protein attrition compared to a standard SWATH acquisition method.
49 Finally, the results showed comparable ability to separate clinical groups.

50

51

52 **Keywords:** SWATH MS; Data-independent Acquisition; FFPE; Biomarker; Prostate cancer
53

54 **INTRODUCTION**

55 A large number of clinical and pre-clinical research questions require biomarkers for the
56 classification of samples or phenotypes. Because they are thought to closely reflect the
57 biochemical state of samples, protein biomarkers are particularly valuable. Protein biomarkers
58 have been intensely sought to indicate disease type or stage, to report disease progression or
59 response or resistance to treatment. For the most part protein biomarker projects use mass
60 spectrometry as the base technique. In spite of enormous research efforts, the number of
61 protein biomarkers discovered by proteomic methods that have progressed to clinical utility
62 remains small (1-4).

63 Protein biomarker discovery and validation projects face significant technical and
64 logistical challenges, including the following: i) biological protein abundance variability.
65 Useful protein biomarkers will only be discovered if the variability within a population is
66 smaller than the variability between protein groups. In the context of a twin cohort study of
67 plasma proteins we have shown that the variability of proteins and the root cause for the
68 variability varies greatly in a human population and that particularly variable proteins are
69 unlikely to be selected as biomarkers (5). ii) confounding effects. Protein biomarker studies
70 suffer from a range of confounding effects, including batch effects of sample collection,
71 sample processing, data acquisition and data analysis. Batch effects are particularly severe
72 among different cohorts that might be required to validate results from a discovery cohort, iii)
73 sample availability. Frequently, sample cohorts of sufficient size and quality to generate
74 sufficient statistical power are not available and iv) technical limitations. Even if suitable
75 cohorts are available acquiring reproducible protein patterns by mass spectrometry from
76 extended cohorts has been costly and challenging. For example, typically, protein biomarkers
77 have multi-dimensional fractionation of the peptides generated from digested, tissue-extracted
78 proteins followed by the analysis of the fractions by shotgun MS analysis. Even if isotopic or
79 isobaric labeling methods increase the multiplexing capability of such analyses (6), the
80 general approach remains expensive and technically challenging (7-9). Overall, these
81 challenges convincingly support the need for the proteomic measurement of large sample
82 cohorts at moderate cost, limited batch effects and high degree of reproducibility. At present
83 state-of-the art, large scale clinical proteomic studies consist of 100 to 200 clinical samples
84 (9-11) and there are indication, *e.g* the lack of stability of discovered marker panels that
85 suggest that this number of samples is at the lower end of the required size range(12). Further,
86 these studies were for the most part carried out by highly specialized groups or consortia
87 using highly optimized analytical platforms. For many proteomic research groups that lack
88 the means to implement the involved consortia methods, meaningful protein biomarker
89 studies have therefore remained out of reach. Therefore, there is an urgent need for robust,
90 highly reproducible, high throughput methods that support large-scale biomarker studies at
91 moderate cost and with limited time consumption.

92 Sample throughput can be increased with short LC gradients for the separation of
93 peptides. Bekker-Jensen et.al have combined multiple dimension pre-fractionation with
94 relatively short LC gradient using shotgun proteomics to achieve deep proteome analysis (13);
95 however, this approach lacks reproducibility and it is still time-consuming for a large cohort
96 study. We and others have found that SWATH/DIA mass spectrometry (14) is a more suitable
97 acquisition method to classify samples in large sample cohorts(5, 15-17). SWATH/DIA is an
98 acquisition method for biomarker studies because it identifies and quantifies peptide
99 precursors via peak groups consisting of fragment ion chromatograms from highly convoluted
100 mass spectra (15) and thus obviates the need to isolate peptide precursors during acquisition.
101 This improves data completeness and enables efficient single-shot proteomic analysis. The
102 key to this MS technique is the ability to collect high-resolution MS/MS spectra at very high
103 acquisition rates, such that a wide mass range can be covered with a series of smaller Q1
104 isolation windows in an LC compatible cycle time. Thus the fast scanning rate of TripleTOF
105 system has been the key in enabling the shortening of LC gradients for analyzing complex
106 tissue proteomes, from 120 min (15) to 45 min (17) without strongly compromising proteome

107 depth, and has been increasingly applied to analyze various types of clinical samples
108 including plasma (5) and tumor tissues (15, 17, 18). A faster nano-LC and Orbitrap-based MS
109 method has been reported recently to allow analysis of plasma and cell line samples using a
110 21-min gradient (19). However, this method requires specialized LC system.

111 To further improve the robustness and throughput of the proteomic analysis of sizable
112 sample cohorts, the use of microflow chromatography is a promising option. An increasing
113 number of studies have demonstrated the applicability of microflow coupled with SWATH
114 MS (20-24). E.g. the Ralser group applied microflow-LC and SWATH to study yeast
115 proteome at a throughput of 60 samples per day (24).

116 Here, we established and optimized a 15-min gradient microflow LC SWATH method,
117 and rigorously examined its performance by analyzing 204 FFPE prostate tissue samples.
118 From the detected 4,043 proteins we prioritized 75 that were further verified with respect to
119 their ability to separate cancer from hyperplasia in an independent FFPE prostate tissue
120 sample cohort study by complementary methods. The results indicate the that short gradient
121 microflow-LC SWATH is a suitable and robust method for clinical protein biomarker studies.

122

123 EXPERIMENTAL PROCEDURES

124 Standard protein digests

125 Digests of proteins isolated from HEK 293 cell were prepared as previously described
126 (25) and provided by Dr Yansheng Liu from ETH Zurich (now in Yale University). Protein
127 digests from K562 cells were obtained from the SWATH Performance Kit (SCIEX). 10% (v/v)
128 iRT peptides (Biognosys, Switzerland) were spiked into peptide samples prior to MS analysis
129 for retention time calibration.

130 PCa patient cohorts and formalin-fixed paraffin-embedded (FFPE) samples

131 Two prostate cancer (PCa) sample cohorts termed PCZA and PCZB were used in this
132 study. The PCZA was acquired by the Second Affiliated Hospital College of Medicine,
133 Zhejiang University and consisted of 58 PCa patients and 10 benign prostatic hyperplasia
134 (BPH) patients. The PCZB cohort was acquired by the Second Affiliated Hospital College of
135 Medicine, Zhejiang University and consisted of 24 PCa patients and 30 BPH patients whose
136 benign and hyperplastic regions have been distinguished. All patients were recruited in 2017
137 and 2018. All cohorts were approved by the ethics committee of the respective hospitals for
138 the procedures of this study.

139 The two different cohort samples were handled by different pathology laboratories, fixed
140 and embedded by the respective staff. The samples were similarly processed and analyzed at
141 different time points. For the PCZA cohort, three biological replicates (size $1 \times 1 \times 5 \text{ mm}^3$)
142 were collected and analyzed by SWATH MS and MRM-HR. For the PCZB cohort, two
143 biological replicates ($1.5 \times 1.5 \times 5 \text{ mm}^3$) were analyzed by MRM-HR.

144 Pressure cycling technology (PCT)-assisted peptide extraction from FFPE tissues

145 About 0.5 mg of FFPE tissue was punched from the samples, weighed and processed for
146 each biological replicate via the FFPE-PCT workflow as described previously (26). Briefly,
147 the tissue punches were first dewaxed by incubating with 1 mL of heptane under gentle
148 vortexing at 600–800 rpm, followed by serial rehydration using 1 mL of 100%, 90%, and 75%
149 ethanol (General reagent, G73537B, Shanghai, China), respectively. The samples were further
150 incubated with 200 μL of 0.1% formic acid (FA) (Thermo Fisher Scientific, T-27563) at 30 °C
151 for 30 min for acidic hydrolysis. The tissue punches were then transferred into
152 PCT-MicroTubes (Pressure Biosciences Inc., Boston, MA, USA, MT-96) and briefly washed
153 with 100 μL of freshly prepared 0.1 M Tris-HCl (pH 10.0) to remove residual FA. Thereafter,
154 the tissues were incubated with 15 μL of freshly prepared 0.1 M Tris-HCl (pH 10.0) at 95 °C

155 for 30 m in with gentle vortexing at 600 rpm. Samples were immediately cooled to 4 °C after
156 basic hydrolysis.

157 Following the pretreatment described above, 25 μ L of lysis buffer including 6 M urea
158 (Sigma, U1230), 2 M thiourea (Amresco, M226) in 100 mM ammonium bicarbonate (General
159 reagent, G12990A, Shanghai, China), pH 8.5 was added to the PCT-MicroTubes containing
160 tissues. The tissue samples were further subjected to PCT-assisted tissue lysis and protein
161 digestion procedures using the Barocycler NEP2320-45K (Pressure Biosciences Inc., Boston,
162 MA, USA) as described previously (27). The PCT scheme for tissue lysis was set with each
163 cycle containing a period of 30 s of high pressure at 45 kpsi and 10 s at ambient pressure,
164 oscillating for 90 cycles at 30°C. Protein reduction and alkylation was performed at ambient
165 pressure by incubating protein extracts with 10 mM Tris(2-carboxyethyl) phosphine (TCEP)
166 (Sigma, C4706) and 20 mM iodoacetamide (IAA) (Sigma, I6125) in darkness at 25 °C for 30
167 min, with gentle vortexing at 600 rpm in a thermomixer. Then the proteins were digested with
168 MS grade Lys-C (Hualishi, Beijing, China, enzyme-to-substrate ratio, 1:40) using a PCT
169 scheme with 50 s of high pressure at 20 kpsi and 10 s of ambient pressure for each cycle,
170 oscillating for 45 cycles at 30 °C. Thereafter, the proteins were further digested with MS
171 grade trypsin (Hualishi, Beijing, China, enzyme-to-substrate ratio, 1:50) using a PCT scheme
172 with 50 s of high pressure at 20 kpsi and 10 s of ambient pressure in one cycle, oscillating for
173 90 cycles at 30 °C. Peptide digests were then acidified with 1% trifluoroacetic (TFA) (Thermo
174 Fisher Scientific, T/3258/PB05) to pH 2–3 and subjected to C18 desalting. iRT peptides were
175 spiked into peptide samples at a final concentration of 10% prior to MS analysis for RT
176 calibration.

177 Optimization of microflow LC gradients coupled with SWATH MS

178 During the optimization studies, 1 μ g peptides were separated with different microflow
179 gradients and different SWATH MS parameters. Linear gradients of 3–35% acetonitrile (0.1%
180 formic acid) with durations of 5, 10, 20, 30, and 45 min were evaluated. The number of Q1
181 variable windows (40, 60, 100) and MS/MS accumulation times (15, 25 ms) constituted the
182 key parameters that were adjusted for the shorter gradients. The need for collision energy
183 spread with the optimized collision energy ramps was tested. Four replicates were performed
184 for each test, after which the data were processed with the PeakView® software with the
185 SWATH 2.0 MicroApp to evaluate the number of proteins and peptides quantified with FDR
186 < 1 % and CV < 20%. The optimized methods were then tested on multiple instruments with
187 different cell lysates to confirm the robustness of the method.

188 SWATH MS acquisition

189 Peptides were separated at a flow rate of 5 μ L/min by a 15-min SWATH of 5–35% linear
190 LC gradient elution (buffer A: 2% ACN (Sigma, 34851), 0.1% formic acid; buffer B: 80%
191 ACN, 0.1% formic acid) on a column, 3 μ m, ChromXP C18CL, 120 Å, 150 x 0.3 mm using
192 an Eksigent NanoLC™ 400 System coupled with a TripleTOF® 6600 system (SCIEX). The
193 DuoSpray Source was replumbed using the 25 μ m ID hybrid electrodes to minimize
194 post-column dead volume. The applied SWATH method was composed of a 150 ms TOF MS
195 scan with m/z ranging from 350 to 1250 Da, followed by MS/MS scans performed on all
196 precursors (from 100 to 1500 Da) in a cyclic manner. A 100 variable Q1 isolation window
197 scheme was used in this study (Supplementary Table 1B). The accumulation time was set at
198 25 ms per isolation window, resulting in a total cycle time of 2.7 s.

199 We also included beta-galactosidase digest (β -gal) (SCIEX, 4465867) for mass and
200 retention time calibration which was analyzed every four injections. The target ion (m/z =
201 729.4) which is from a peptide precursor in the β -gal digest mixture was monitored under
202 high sensitivity mode. The RT, intensity, and m/z of targeted precursor and fragment ions
203 were respectively used for LC QC, the sensitivity test, and mass calibration separately.

204 MRM-HR MS acquisition

205 A time scheduled MRM-HR targeted quantification strategy was used to further validate
206 proteins observed to be differentially expressed proteins by SWATH MS as described above.
207 The same microflow LC approach was used for 15-min SWATH MS analysis. The TripleTOF
208 6600 mass spectrometer was operated in IDA mode for time-scheduling the MS/MS
209 acquisition for 134 peptides for the MRM-HR workflow. The method consisted of one 75 ms
210 TOF-MS scan for precursor ions with m/z ranging from 350 to 1250 Da, followed by MS/MS
211 scans for fragment ions with m/z ranging from 100 to 1500 Da, allowing for a maximum of
212 45 candidate ions being monitored per cycle (25 ms accumulation time, 50 ppm mass
213 tolerance, rolling collision energy, +2 to +5 charge states with intensity criteria above 2 000
214 000 cps to guarantee that no untargeted peptides should be acquired). The fragment ion
215 information including m/z and RT of a targeted precursor ion was confirmed by previous
216 SWATH results and was then added to the inclusion list for the targeted analysis. The intensity
217 threshold of targeted precursors in the inclusion list was set to 0 cps and the scheduling
218 window was 60 s. The targeted peptide sequences were the same as those found in the
219 previous SWATH MS analysis.

220 Targeted MRM-HR data were analyzed by 19.0.9.149 Skyline (28), which automatically
221 detected the extracted-ion chromatogram (XIC) from an LC run by matching the MS spectra
222 of the targeted ion against its spectral library generated from the IDA mode within a specific
223 mass tolerance window around its m/z. All peaks selected were checked manually after
224 automated peak detection using Skyline. Both MS1 and MS2 filtering were set as “TOF mass
225 analyzer” with a resolution power of 30 000 and 15 000, respectively, while the “Targeted”
226 acquisition method was defined in the MS/MS filtering.

227 SWATH data analysis

228 The optimization data for optimal LC gradients were processed using the SWATH 2.0
229 MicroApp in PeakView® software (SCIEX) using the pan-human library (29). RT calibration
230 was performed by first using iRT peptides with RT window at a 75 ppm XIC extraction width.
231 Replicate analysis was performed using the SWATH Replicate Analysis Template (SCIEX) to
232 determine the number of peptides and proteins quantified with FDR < 1% peptide and CV <
233 10 or 20%.

234 The data from prostate samples were processed using the OpenSWATH pipeline. Briefly,
235 SWATH raw data files were converted in profile mode to mzXML using msconvert and
236 analyzed using OpenSWATH (2.0.0) (30) as described previously (15). The retention time
237 extraction window was 600 s, while m/z extraction was performed with 0.03 Da tolerance. RT
238 was then calibrated using both iRT peptides. Peptide precursors were identified by
239 OpenSWATH and PyProphet (2.0.1) with d_score < 0.01 and FDR < 1%. For each protein,
240 the median MS2 intensity value of peptide precursor fragments which were detected to belong
241 to the protein was used to represent the protein abundance.

242

243 RESULTS AND DISCUSSIONS

244 Establishment and optimization of the 15-min microflow SWATH MS method

245 A HEK 293 cell lysate digest was used to establish and optimize the short microflow LC
246 gradient and SWATH acquisition schemes on TripleTOF 6600 systems. Specifically, we tested
247 the effects of LC gradient lengths of 5, 10, 20, and 45 min, and mass spectrometer parameters
248 including variable Q1 windows and accumulation time for MS2 (Supplementary Table 1). For
249 each injection 1 µg mass of total peptide was loaded onto a microflow column of 150 x 0.3
250 mm dimensions and analyzed under a range of conditions. To increase robustness of results,
251 four technical replicates of each condition were used. The acquired data were searched
252 consistently searched against PHL with the PeakView® software and the SWATH 2.0
253 MicroApp and the number of peptides and inferred proteins, as well as their intensities were
254 recorded. The data was processed as described in the methods section and evaluated

255 according to the number of proteins and peptides identified with FDR < 1% and quantified
256 with CV < 10% or CV < 20%, respectively. The whole dataset was acquired on two different
257 instruments. Supplementary Figure 1a shows that using shorter gradient methods generated
258 similar results between the two different 6600 instruments. Our data also showed that the 20
259 min microflow method detected 90% of the proteins quantified by 45 min method, while the
260 10 min LC method identified 70% of the proteins. With decreasing gradient length, the
261 number of identified proteins further decreased to 77% for a 10 min method to 53% for a 5
262 min method in their best condition (Supplementary Figure 1a).

263 Next, we optimized the specific mass spec parameters including variable windows and
264 accumulation times to balance the width of the windows and scan times (Supplementary
265 Figure 1b). Typically, more variable windows led to more peptides and proteins quantified
266 robustly, but only up to a point where the MS/MS acquisition rates become too fast or the
267 cycle times too long, as evidenced in the 5min gradient optimization results. Thus, a higher
268 number of variable windows led to a higher number of peptide and protein identifications.
269 The optimal accumulation time was highly dependent on the LC time. Higher numbers of
270 acquisition windows necessitated shorter MS/MS accumulation times per precursor ion
271 window to maintain a cycle time that was compatible with the peak width generated by the
272 respective gradients. Considering the tradeoff between sample throughput and numbers of
273 proteins quantified, the gradient time from 10 min to 20 min is a better choice according to
274 the efficiency of peptides and proteins identification in unit of time (Supplementary Figure
275 1b). Therefore, we chose the 15 min gradient as the optimal LC condition (Supplementary
276 Figure 2).

277 **Application of short gradient microflow-SWATH to a PCa patient cohort**

278 We evaluated the performance of the optimized short gradient microflow LC SWATH
279 method on a set of prostate cancer (PCa) tissue samples named PCZA. The set consisted of
280 204 FFPE biospecimens collected from 58 PCa patients and 10 benign hyperplasia (BPH)
281 patients (Supplementary Table 2) for which clinical data were also available. The 204 samples
282 were randomly divided into seven batches and digested into peptides in barocyclers. Every
283 batch included a mouse liver sample as quality control (QC) for the PCT-assisted sample
284 preparation and a prostate tissue pool samples as the QC sample for SWATH MS
285 (Supplementary Figure 3).

286 We then subjected the resulting peptide samples to the 15-min-SWATH method optimized
287 above (Figure 1a). The total sample set consisted of 58 PCa samples and 7 QC and reference
288 samples. The 204 samples were measured in 125.7 hrs (~5 days) and quantified 27,975
289 peptide precursors from 4,038 SwissProt proteins (without protein grouping) with 74.79%
290 missing value rate. On average, 5,615 peptide precursors from 1,018 proteins were quantified
291 for each sample. More peptides and proteins were quantified from tumor samples (5,861
292 peptide precursors from 1,078 proteins on average) than benign samples (3,988 peptide
293 precursors from 618 proteins on average). Totally 913 proteins were quantified in at least 50%
294 samples (Supplementary Table 3).

295 To allow a comparison of the accelerated short gradient method with a standard SWATH
296 MS method with respect to the number of proteins recorded and the respective clinically
297 relevant information content we re-acquired the whole sample set with a 120-min LC gradient
298 and 48 variable Q1 windows in a TripleTOF 5600+(26). These measurements consumed 467
299 hr (~20 days) and identified 38,338 peptide precursors from 5,059 SwissProt proteins with
300 61.86% missing value rate. On average, 10,751 peptide precursors from 1,921 proteins were
301 quantified for each sample. More peptides and proteins were quantified from tumor samples
302 (11,439 peptide precursors from 2,054 proteins on average) than benign samples (6,693
303 peptide precursors from 1192 proteins on average). Totally 1,914 proteins were quantified in
304 at least 50% samples (Supplementary Table 3). Compare to this 120-min method, the 15-min
305 method characterized about half of peptide precursors and proteins.
306

307 Overall, the data shows that the 15-min-SWATH coverage reached 50-80% of that
308 achieved by a standard method. In all samples, 3,800 proteins were quantified by both
309 methods. This result was generated at a 6-fold reduced acquisition time (time 125.7 hrs vs,
310 467 hrs) (Figure 1b) suggesting that clinical cohorts of significant size can be measured by the
311 accelerated method quickly, efficiently.

312 **Reproducibility and batch effect analysis**

313 We evaluated the reproducibility of the datasets produced by the 15-min gradient and the 120-
314 min gradient SWATH with respect to reproducibility and batch effect. We first assessed the
315 technical reproducibility by correlation between technical replicates for LC-MS. The
316 technical reproducibility of the data obtained by the 15-min SWATH method ($r = 0.99$) is
317 slightly higher than that from the 120-min SWATH method ($r = 0.86$) (Figure 2a). Thus, the
318 measured biological reproducibility is also slightly higher in the 15-min SWATH method
319 (Figure 2a). If we focused the analysis on the 3,800 proteins quantified by both methods, we
320 observed a high degree of similarity ($r = 0.7681$) between the methods (Figure 2b).

321 We next analyzed batch effects apparent in either dataset. Batch effects are an
322 unavoidable reality resulting from technical variation in multi-day MS analyses and are a
323 non-trivial complication for big cohort proteomics analysis. Several algorithms have been
324 developed to bioinformatically minimize the missing value rate, however, these imputation
325 approaches remain controversial (31). We evaluated the batch effect of the data acquired by
326 the 15-min SWATH, which is lower than that from the 120-min method (Figure 2c). Together,
327 the 15-min SWATH method improved quantitative reproducibility and reduced batch effect.
328

329 **Verification of differential expression proteins using MRM-HR**

330 On the path to clinical or preclinical use protein biomarkers detected by MS based cohort
331 studies face a number of verification and validation requirements. These include technical
332 verification of the abundance changes detected in the cohort study and validation in
333 independent sample cohorts.

334 To further validation the abundance changes detected in the SWATH data we selected a
335 panel of 75 proteins showing different abundance (absolute fold change larger than two and
336 adjusted p-value less than 0.05) between control and tumor tissue and measured their
337 respective intensities using the targeted MS method MRM-HR. The selected proteins were
338 associated with most strongly cancer dis regulated pathways and included 21 known
339 diagnosis biomarkers such as ACPP and FASN, and 10 drug targets (Supplementary Table
340 4A). The proteins were further annotated in IPA (Supplementary Table 4B) indicating that the
341 proteins suggested elevated cell migration, development and growth, and suppressed cell
342 death and survival (Supplementary Figure 5).

343 For these measurements the MRM-HR method was optimized using a pooled prostate
344 sample to determine the best performing peptides from the selected proteins, and best target
345 fragment ions for quantitation. The information about proteins and peptides including the RTs
346 was imported into Skyline to build a spectral library. A total of 134 peptides for 75 proteins
347 were selected for targeted detection (Supplementary Table 2E). Time scheduling was used to
348 ensure at least eight data points were obtained across the LC peaks as well as an optimized
349 accumulation time of 25 ms for each peptide for high-quality quantitative data.

350 To confirm the quantitative accuracy of the 15-min SWATH data, we re-analyzed 99
351 samples in the PCZA cohort using the MRM-HR method. The 99 samples were randomly
352 allocated to five batches, each containing 20 samples and an extra MS QC sample which was
353 a pool of prostate tissue digests in PCZA. We firstly examined the reproducibility of XICs for
354 all peptides in MRM-HR assays. For the five pooled samples measured across five batches,
355 we found that 76.6% of precursors measured from the peptides were quantified with a CV
356 below 20%. The median CV was 13.4% (Supplementary Figure 6). Next the protein
357 fold-changes between tumor and normal samples were calculated to investigate the

358 correlation of 15-min SWATH with MRM-HR (Figure 3a).

359 We further quantified the expression levels of the 75-protein-panel in an independent
360 prostate cancer cohort, PCZB, containing 30 BPH and 24 PCa in duplicated biological
361 replicates using the same 15-min SWATH MRM-HR workflow (Supplementary Table 5). For
362 the six pooled samples measured across six batches, 75.6% of peptide precursors were
363 quantified with a CV below 20%. The median CV is 14.9% (Supplementary Figure 6).

364 To assess the power of the protein panel of differentially abundant proteins to separate
365 benign and malignant tissues, we assembled a random-forest model for the PCZA MRM-HR
366 dataset, and found an accuracy of 0.992 in this set (Supplementary Figure 7). Next, we tested
367 the ability of this panel to separate tumor from benign prostatic tissue samples in an
368 independent patient group, *i.e.* PCZB, including 24 PCa patients and 30 BPH patients. The
369 receiver operating curves (ROC) of the 75-protein-panel clearly distinguished PCa from BPH
370 patient groups (Figure 3b).

371 We then investigated in detail two proteins—PRDX3 (P30048) and COPA (P53621) which
372 were prioritized because of their role in TP53 oncogene regulation and as a potential drug
373 (decitabine) target (Supplementary Figure 8). The data show that these proteins significantly
374 up-regulated in tumor tissue from all three workflows, *i.e.* 15-min-SWATH, and MRM-HR in
375 the PCZA cohort samples and MRM-HR in the PCZB cohort (Figure 3b). The ROC curve of
376 these two proteins from three different datasets distinguishing benign from malignant tissue
377 samples are shown in Supplementary Figure 9, with all of AUC over 0.78. Taken together, we
378 validated these dysregulated proteins quantification by SWATH showed higher reliability and
379 performed better prediction ability in different sample cohorts.

380

381 Conclusion

382 In this study, we present a 15-min microflow-LC SWATH that supports the consistent
383 proteomic analysis of clinical (FFPE) samples at a throughput of ~50 samples per day
384 (excluding calibration and washing). The method is therefore well suited for the analysis of
385 large sample cohorts, even in a single investigator proteomic laboratory. The results show that
386 the presented method increases the throughput by ca six-fold compared to a conventional
387 SWATH MS method, at reduced batch effects and at an attrition of ca 20% of detected
388 proteins and increased missing value rate (~20% worse) in the prostate cancer cohort. For
389 individual samples, the number of detected proteins decreased by ~50%. The quantitative
390 accuracy of the short gradient method was comparable to that achieved by targeted
391 quantification using MRM-HR for shortlisted proteins. This work showed the potential of this
392 short gradient SWATH proteomics pipeline for accelerated discovery and verification of
393 protein biomarkers for precision medicine.

394 Author Contributions

395 T.G., C.H., R.S. designed the project. C.H., N.M. and C.C. optimized the 15-min-SWATH.
396 X.Y., L.C. procured the three prostate cohorts. R.S. performed the PCT SWATH analysis with
397 help from X.C. C.C. and R.S. performed the MRM-HR analysis. W.G., R.S., S.D., analyzed
398 the data. R.S., Y.Z., C.H., R.A. and T.G. wrote the manuscript. Z.L assisted data analysis. S.L.,
399 C.Y. gave valuable advice. T.G., Y.Z. supported and supervised the project.

400

401 **Research Funding:** Zhejiang Provincial Natural Science Foundation of China (Grant No.
402 LR19C050001 to T.G.). Hangzhou Agriculture and Society Advancement Program (Grant No.
403 20190101A04 to T.G.). National Natural Science Foundation of China (General Program)
404 (Grant No. 81972492 to T.G.). National Science Fund for Young Scholars (Grant No.
405 21904107).

406

407 **Acknowledgments:** We thank Dr Xuan Ding for review of the manuscript.

408 **Competing financial interests:** The research group of T.G. is partly supported by SCIEX,
409 which provides access to prototype instrumentation, and Pressure Biosciences Inc, which
410 provides access to advanced sample preparation instrumentation.

411
412 **Data and materials availability:** The 15-min SWATH data are deposited in PRIDE. Project
413 accession: IPX0001645000. The 15-min SWATH data are deposited in iProX
414 (IPX0001645001). The MRM-HR data are deposited in iProX (IPX0001645002). All the data
415 will be publicly released upon publication.

416

417 **ABBREVIATIONS**

418 AUC = area under the curve

419 BPH = benign prostatic hyperplasia

420 CV = coefficient of variation

421 DDA = data dependent acquisition

422 DIA = data independent acquisition

423 FA = formic acid

424 FDR = false discovery rate

425 FFPE = formalin fixed, paraffin embedded

426 IAA = iodoacetamide

427 IPA = ingenuity pathway analysis

428 LC = liquid chromatograph

429 MRM-HR = multiple reaction monitoring high-resolution

430 PCa = prostate cancer

431 PCT = pressure cycling technology

432 PRM = parallel reaction monitoring

433 QC = quality control

434 ROC = receiver operating characteristic

435 RF = random forest

436 RT = retention time

437 SWATH MS = sequential windowed acquisition of all theoretical fragment ion - mass spectra

438 TCEP = tris(2-carboxyethyl) phosphineTFA = trifluoroacetic

439 TMA = tissue microarray analysis

440 TOF = time of flight

441 XIC = extracted ion chromatogram

442

443 **References**

444 1. Olsen, M.; Ghannad, M.; Lok, C.; Bossuyt, P. M., Shortcomings in the evaluation of

445 biomarkers in ovarian cancer: a systematic review. *Clin Chem Lab Med* **2019**.

446 2. Rifai, N.; Gillette, M. A.; Carr, S. A., Protein biomarker discovery and validation: the long

447 and uncertain path to clinical utility. *Nat Biotechnol* **2006**, 24, (8), 971-83.

448 3. Anderson, N. L.; Ptolemy, A. S.; Rifai, N., The riddle of protein diagnostics: future bleak or
449 bright? *Clin Chem* **2013**, 59, (1), 194-7.

450 4. Frantzi, M.; Latosinska, A.; Kontostathi, G.; Mischak, H., Clinical Proteomics: Closing the
451 Gap from Discovery to Implementation. *Proteomics* **2018**, 18, (14), e1700463.

452 5. Liu, Y.; Buil, A.; Collins, B. C.; Gillet, L. C.; Blum, L. C.; Cheng, L. Y.; Vitek, O.; Mouritsen,
453 J.; Lachance, G.; Spector, T. D.; Dermitzakis, E. T.; Aebersold, R., Quantitative variability of
454 342 plasma proteins in a human twin population. *Mol Syst Biol* **2015**, 11, (1), 786.

455 6. Aebersold, R.; Mann, M., Mass-spectrometric exploration of proteome structure and
456 function. *Nature* **2016**, 537, (7620), 347-55.

457 7. Sabrkhany, S.; Kuijpers, M. J. E.; Knol, J. C.; Olde Damink, S. W. M.; Dingemans, A. C.;
458 Verheul, H. M.; Piersma, S. R.; Pham, T. V.; Griffioen, A. W.; Oude Egbrink, M. G. A.; Jimenez,
459 C. R., Exploration of the platelet proteome in patients with early-stage cancer. *J Proteomics*
460 **2018**, 177, 65-74.

461 8. Mun, D. G.; Bhin, J.; Kim, S.; Kim, H.; Jung, J. H.; Jung, Y.; Jang, Y. E.; Park, J. M.; Kim,
462 H.; Jung, Y.; Lee, H.; Bae, J.; Back, S.; Kim, S. J.; Kim, J.; Park, H.; Li, H.; Hwang, K. B.; Park,
463 Y. S.; Yook, J. H.; Kim, B. S.; Kwon, S. Y.; Ryu, S. W.; Park, D. Y.; Jeon, T. Y.; Kim, D. H.; Lee,
464 J. H.; Han, S. U.; Song, K. S.; Park, D.; Park, J. W.; Rodriguez, H.; Kim, J.; Lee, H.; Kim, K. P.;
465 Yang, E. G.; Kim, H. K.; Paek, E.; Lee, S.; Lee, S. W.; Hwang, D., Proteogenomic
466 Characterization of Human Early-Onset Gastric Cancer. *Cancer Cell* **2019**, 35, (1), 111-124
467 e10.

468 9. Zhang, H.; Liu, T.; Zhang, Z.; Payne, S. H.; Zhang, B.; McDermott, J. E.; Zhou, J. Y.;
469 Petyuk, V. A.; Chen, L.; Ray, D.; Sun, S.; Yang, F.; Chen, L.; Wang, J.; Shah, P.; Cha, S. W.;

470 Aiyetan, P.; Woo, S.; Tian, Y.; Gritsenko, M. A.; Clauss, T. R.; Choi, C.; Monroe, M. E.;

471 Thomas, S.; Nie, S.; Wu, C.; Moore, R. J.; Yu, K. H.; Tabb, D. L.; Fenyö, D.; Bafna, V.; Wang,

472 Y.; Rodriguez, H.; Boja, E. S.; Hiltke, T.; Rivers, R. C.; Sokoll, L.; Zhu, H.; Shih, I. M.; Cope, L.;

473 Pandey, A.; Zhang, B.; Snyder, M. P.; Levine, D. A.; Smith, R. D.; Chan, D. W.; Rodland, K. D.;

474 Investigators, C., Integrated Proteogenomic Characterization of Human High-Grade Serous

475 Ovarian Cancer. *Cell* **2016**, 166, (3), 755-765.

476 10. Vasaikar, S.; Huang, C.; Wang, X.; Petyuk, V. A.; Savage, S. R.; Wen, B.; Dou, Y.; Zhang,

477 Y.; Shi, Z.; Arshad, O. A.; Gritsenko, M. A.; Zimmerman, L. J.; McDermott, J. E.; Clauss, T. R.;

478 Moore, R. J.; Zhao, R.; Monroe, M. E.; Wang, Y. T.; Chambers, M. C.; Slebos, R. J. C.; Lau, K.

479 S.; Mo, Q.; Ding, L.; Ellis, M.; Thiagarajan, M.; Kinsinger, C. R.; Rodriguez, H.; Smith, R. D.;

480 Rodland, K. D.; Liebler, D. C.; Liu, T.; Zhang, B.; Clinical Proteomic Tumor Analysis, C.,

481 Proteogenomic Analysis of Human Colon Cancer Reveals New Therapeutic Opportunities.

482 *Cell* **2019**, 177, (4), 1035-1049 e19.

483 11. Mertins, P.; Mani, D. R.; Ruggles, K. V.; Gillette, M. A.; Clauser, K. R.; Wang, P.; Wang,

484 X.; Qiao, J. W.; Cao, S.; Petralia, F.; Kawaler, E.; Mundt, F.; Krug, K.; Tu, Z.; Lei, J. T.; Gatza,

485 M. L.; Wilkerson, M.; Perou, C. M.; Yellapantula, V.; Huang, K. L.; Lin, C.; McLellan, M. D.; Yan,

486 P.; Davies, S. R.; Townsend, R. R.; Skates, S. J.; Wang, J.; Zhang, B.; Kinsinger, C. R.; Mesri,

487 M.; Rodriguez, H.; Ding, L.; Paulovich, A. G.; Fenyö, D.; Ellis, M. J.; Carr, S. A.; Nci, C.,

488 Proteogenomics connects somatic mutations to signalling in breast cancer. *Nature* **2016**, 534,

489 (7605), 55-62.

490 12. Thomas, S.; Friedrich, B.; Schnaubelt, M.; Chan, D.; Zhang, H.; Aebersold, R.,

491 Orthogonal proteomic platforms and their implications for the stable classification of

492 high-grade serous ovarian cancer subtypes. *BioRxiv* **2019**.

493 13. Bekker-Jensen, D. B.; Kelstrup, C. D.; Batth, T. S.; Larsen, S. C.; Haldrup, C.; Bramsen, J.

494 B.; Sorensen, K. D.; Hoyer, S.; Orntoft, T. F.; Andersen, C. L.; Nielsen, M. L.; Olsen, J. V., An

495 Optimized Shotgun Strategy for the Rapid Generation of Comprehensive Human Proteomes.

496 *Cell Syst* **2017**, 4, (6), 587-599 e4.

497 14. Gillet LC, N. P., Tate S, Röst H, Selevsek N, Reiter L, Bonner R, Aebersold R., Targeted

498 data extraction of the MS/MS spectra generated by data-independent acquisition: a new

499 concept for consistent and accurate proteome analysis. *Mol Cell Proteomics*. **2012**.

500 15. Guo, T.; Kouvonen, P.; Koh, C. C.; Gillet, L. C.; Wolski, W. E.; Rost, H. L.; Rosenberger,

501 G.; Collins, B. C.; Blum, L. C.; Gillessen, S.; Joerger, M.; Jochum, W.; Aebersold, R., Rapid

502 mass spectrometric conversion of tissue biopsy samples into permanent quantitative digital

503 proteome maps. *Nat Med* **2015**, 21, (4), 407-13.

504 16. Bouchal, P.; Schubert, O. T.; Faktor, J.; Capkova, L.; Imrichova, H.; Zoufalova, K.;

505 Paralova, V.; Hrstka, R.; Liu, Y.; Ebhardt, H. A.; Budinska, E.; Nenutil, R.; Aebersold, R.,

506 Breast Cancer Classification Based on Proteotypes Obtained by SWATH Mass Spectrometry.

507 *Cell Rep* **2019**, 28, (3), 832-843 e7.

508 17. Zhu, Y.; Zhu, J.; Lu, C.; Zhang, Q.; Xie, W.; Sun, P.; Dong, X.; Yue, L.; Sun, Y.; Yi, X.; Zhu,

509 T.; Ruan, G.; Aebersold, R.; Huang, S.; Guo, T., Identification of Protein Abundance Changes

510 in Hepatocellular Carcinoma Tissues Using PCT-SWATH. *Proteomics Clin Appl* **2019**, 13, (1),

511 e1700179.

512 18. Guo, T.; Li, L.; Zhong, Q.; Rupp, N. J.; Charmpi, K.; Wong, C. E.; Wagner, U.; Rueschoff,

513 J. H.; Jochum, W.; Fankhauser, C. D.; Saba, K.; Poyet, C.; Wild, P. J.; Aebersold, R.; Beyer, A.,

514 Multi-region proteome analysis quantifies spatial heterogeneity of prostate tissue biomarkers.

515 *Life Sci Alliance* **2018**, 1, (2).

516 19. Bache N1, G. P., 3, Bekker-Jensen DB3, Hoerning O1, Falkenby L1, Treit PV2, Doll S2,

517 Paron I2, Müller JB2, Meier F2, Olsen JV3, Vorm O1, Mann M, A Novel LC System Embeds

518 Analytes in Pre-formed Gradients for Rapid, Ultra-robust Proteomics. *Mol Cell Proteomics*.

519 **2018**.

520 20. Shi, J.; Wang, X.; Lyu, L.; Jiang, H.; Zhu, H. J., Comparison of protein expression

521 between human livers and the hepatic cell lines HepG2, Hep3B, and Huh7 using SWATH and

522 MRM-HR proteomics: Focusing on drug-metabolizing enzymes. *Drug Metab Pharmacokinet*

523 **2018**, 33, (2), 133-140.

524 21. He, B.; Shi, J.; Wang, X.; Jiang, H.; Zhu, H. J., Label-free absolute protein quantification

525 with data-independent acquisition. *J Proteomics* **2019**, 200, 51-59.

526 22. Colgrave, M. L.; Byrne, K.; Blundell, M.; Heidelberger, S.; Lane, C. S.; Tanner, G. J.;

527 Howitt, C. A., Comparing Multiple Reaction Monitoring and Sequential Window Acquisition of

528 All Theoretical Mass Spectra for the Relative Quantification of Barley Gluten in Selectively

529 Bred Barley Lines. *Anal Chem* **2016**, 88, (18), 9127-35.

530 23. Le Duff, M.; Gouju, J.; Jonchere, B.; Guillon, J.; Toutain, B.; Boissard, A.; Henry, C.;

531 Guette, C.; Lelievre, E.; Coqueret, O., Regulation of senescence escape by the

532 cdk4-EZH2-AP2M1 pathway in response to chemotherapy. *Cell Death Dis* **2018**, 9, (2), 199.

533 24. Vowinckel, J.; Zelezniak, A.; Bruderer, R.; Mulleder, M.; Reiter, L.; Ralser, M.,

534 Cost-effective generation of precise label-free quantitative proteomes in high-throughput by

535 microLC and data-independent acquisition. *Sci Rep* **2018**, 8, (1), 4346.

536 25. Liu, Y.; Mi, Y.; Mueller, T.; Kreibich, S.; Williams, E. G.; Van Drogen, A.; Borel, C.; Frank,
537 M.; Germain, P. L.; Bludau, I.; Mehnert, M.; Seifert, M.; Emmenlauer, M.; Sorg, I.; Bezrukov, F.;
538 Bena, F. S.; Zhou, H.; Dehio, C.; Testa, G.; Saez-Rodriguez, J.; Antonarakis, S. E.; Hardt, W.
539 D.; Aebersold, R., Multi-omic measurements of heterogeneity in HeLa cells across laboratories.
540 *Nat Biotechnol* **2019**, 37, (3), 314-322.

541 26. Yi Zhu 1, 3*, Tobias Weiss 4*, Qiushi Zhang 1,2, Rui Sun 1,2, Bo Wang 5, Zhicheng Wu
542 1,2, Qing Zhong 6,7, Xiao Yi 1,2 , Huanhuan Gao 1,2, Xue Cai 1,2, Guan Ruan 1,2, Tiansheng
543 Zhu 1,2, Chao Xu , Sai Lou 9, Xiaoyan Yu 10, Ludovic Gillet 3, Peter Blattmann 3, Karim Saba
544 11, Christian D.Fankhauser 11, Michael B. Schmid 11, Dorothea Rutishauser 6, Jelena
545 Ljubicic 6, Ailsa , Christiansen 6, Christine Fritz 6, Niels J. Rupp 6, Cedric Poyet 11, Elisabeth
546 Rushing 12, Michael Weller 4, Patrick Roth 4, Eugenia Haralambieva 6, Silvia Hofer 13, Chen
547 Chen 14, Wolfram Jochum 15, Xiaofei Gao 1,2, Xiaodong Teng 5, Lirong Chen 10, Peter J.
548 Wild 6,16#, Ruedi Aebersold 3,17# , Tiannan Guo, High-throughput proteomic analysis of
549 FFPE tissue samples facilitates tumor stratification. *bioRxiv* **2019**.

550 27. Zhu, Y.; Guo, T., High-Throughput Proteomic Analysis of Fresh-Frozen Biopsy Tissue
551 Samples Using Pressure Cycling Technology Coupled with SWATH Mass Spectrometry.
552 *Methods Mol Biol* **2018**, 1788, 279-287.

553 28. MacLean, B.; Tomazela, D. M.; Shulman, N.; Chambers, M.; Finney, G. L.; Frewen, B.;
554 Kern, R.; Tabb, D. L.; Liebler, D. C.; MacCoss, M. J., Skyline: an open source document editor
555 for creating and analyzing targeted proteomics experiments. *Bioinformatics* **2010**, 26, (7),
556 966-8.

557 29. Rosenberger, G.; Koh, C. C.; Guo, T.; Rost, H. L.; Kouvonen, P.; Collins, B. C.; Heusel,

558 M.; Liu, Y.; Caron, E.; Vichalkovski, A.; Faini, M.; Schubert, O. T.; Faridi, P.; Ebhardt, H. A.;

559 Matondo, M.; Lam, H.; Bader, S. L.; Campbell, D. S.; Deutsch, E. W.; Moritz, R. L.; Tate, S.;

560 Aebersold, R., A repository of assays to quantify 10,000 human proteins by SWATH-MS. *Sci*

561 *Data* **2014**, 1, 140031.

562 30. Rost, H. L.; Rosenberger, G.; Navarro, P.; Gillet, L.; Miladinovic, S. M.; Schubert, O. T.;

563 Wolski, W.; Collins, B. C.; Malmstrom, J.; Malmstrom, L.; Aebersold, R., OpenSWATH enables

564 automated, targeted analysis of data-independent acquisition MS data. *Nat Biotechnol* **2014**,

565 32, (3), 219-23.

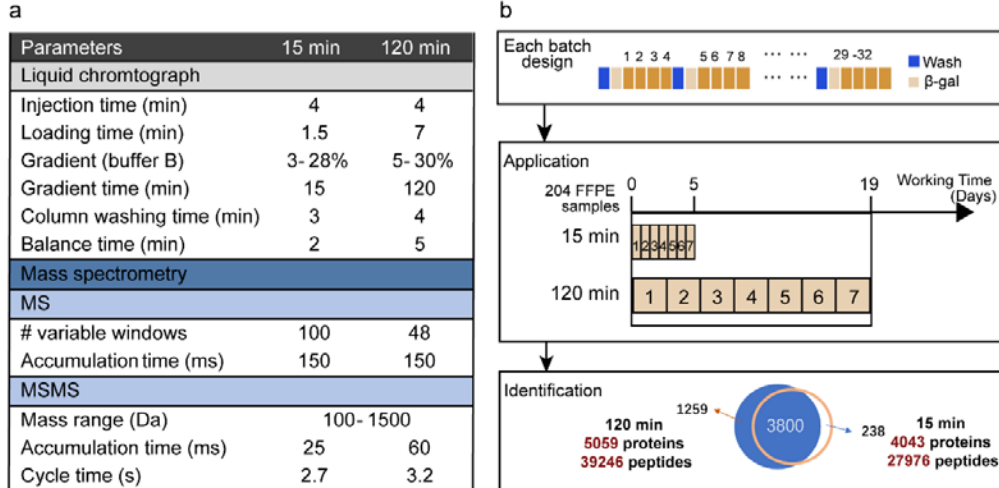
566 31. Goh, W. W. B.; Wong, L., Advanced bioinformatics methods for practical applications in

567 proteomics. *Brief Bioinform* **2019**, 20, (1), 347-355.

568

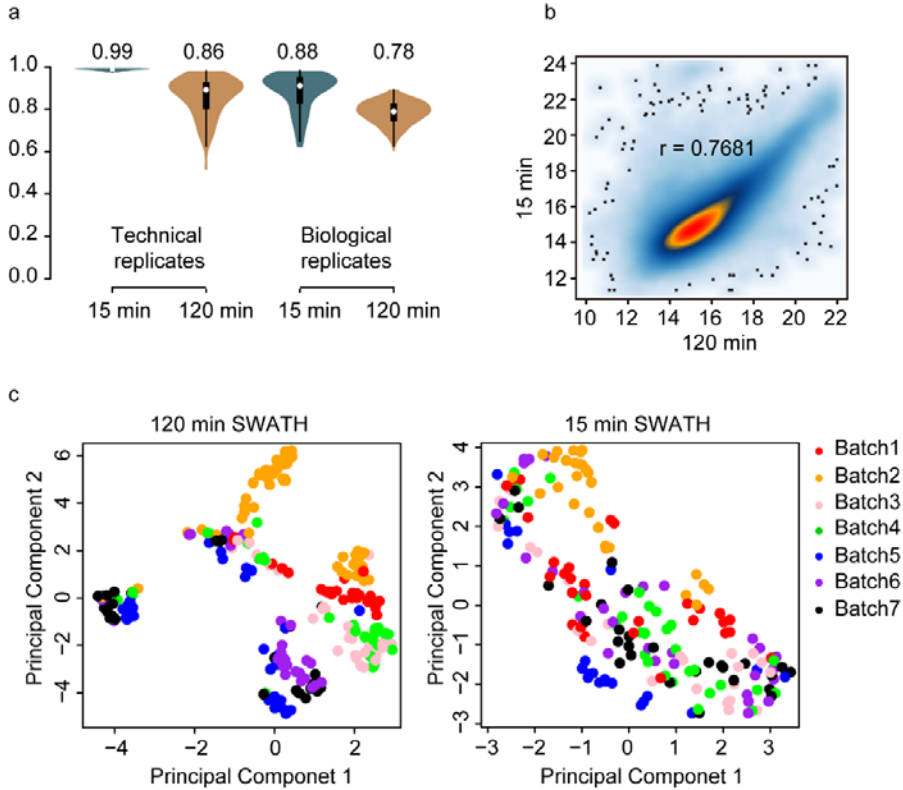
569

570 Figure 1. The short-gradient SWATH method and application in the PCZA PCa cohort. (a)
571 Comparison of parameters between the 15-min SWATH and 120-min SWATH methods. (b)
572 The workflow of the 15-min-SWATH and conventional SWATH for the PCZA cohort. We
573 designed seven randomly shuffled batches with a column washing run and a calibration (β -gal)
574 run inserted every four samples.



575
576

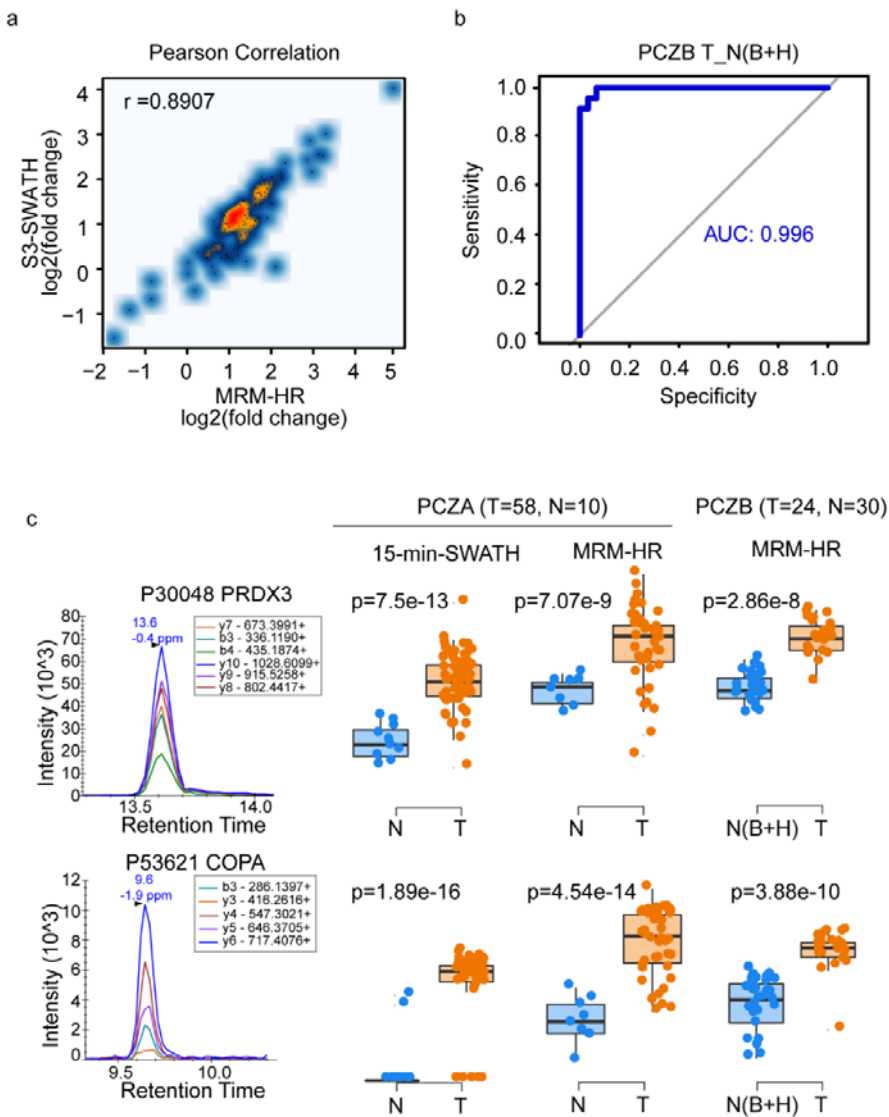
577 Figure 2. The reproducibility of the short gradient SWATH method in the PCZA PCa cohort.
578 (a) Violin plots show the technical replicates and biological replicates in the two methods. (b)
579 Pearson correlation of log2-scaled protein intensity values obtained from 3,800 proteins that
580 were quantified by both methods. (c) PCA analysis of all samples quantified by the 120-min
581 method (left) and the 15-min method (right).



582

583

584 Figure 3. Verification of proteomic data using MRM-HR. (a) Pearson correlation coefficient
585 between the 15-min SWATH and MRM-HR datasets based on the $\log_2(T/N)$ of protein
586 expression in PCZA. (b) The ROC curves of protein quantification from MRM-HR to predict
587 the tumor and normal tissues with the random forest algorithm in PCZB (T: PCa, N: BPH, H:
588 hyperplasia in BPH patients, B: benign in BPH patients). (c) MRM-HR validation of potential
589 diagnostic proteins using the PCZA and PCZB. PRDX3 (peptide: +2 DYGVVLLEGSGLALR),
590 COPA (peptide: +2 DVAVMQLR). The left panel shows the fragment ion extracted-ion
591 chromatograms (XICs) for the peptide from each protein. The right panel of boxplots shows
592 the peptides quantified in the different data sets.



593